JOURNAL OF Materials CHEMISTRY

Tetraaryl biphenyl diamine hole transport materials: a structural study utilizing both single crystal and high resolution powder diffraction

Alan R. Kennedy,*[a] W. Ewen Smith,[a] Daniel R. Tackley,[a] William I. F. David,[b] Kenneth Shankland,[b] Bev Brown[c] and Simon J. Teat[d]

[a]*Department of Pure and Applied Chemistry, University of Strathclyde, Glasgow, Scotland, UK G1 1XL. E-mail: a.r.kennedy@strath.ac.uk; Fax: 0141 552 0876; Tel: 0141 548 2016*
[b]*ISIS Facility, CLRC Rutherford Appleton Laboratory, Chilton, Oxfordshire, England, UK OX11 0QX*
[c]*Avecia Ltd., PO Box 42, Hexagon House, Blackley, Manchester, England, UK M9 8ZS*
[d]*CLRC Daresbury Laboratory, Warrington, England, UK WA4 4AD*

Received 10th August 2001, Accepted 13th November 2001
First published as an Advance Article on the web 20th December 2001

The use of synchrotron based instruments has allowed the crystal structures of the triarylamine based hole transport materials *N*,*N*′-diphenyl-*N*,*N*′-bis(3-methylphenyl)-1,1′-biphenyl-4,4′-diamine (TPD) and *N*,*N*′-diphenyl-*N*,*N*′-bis(4-methylphenyl)-1,1′-biphenyl-4,4′-diamine (TPD-4) to be determined for the first time. The structure of TPD, based on a single crystal experiment using a microcrystal, has profound implications for work on elucidating the hole transport mechanism of these materials as it is shown to contain two disordered but distinct molecular conformations. Neither conformation corresponds to previous predictions from density functional theory. Further complicating the system is the presence of a second polymorph detected in bulk TPD. The crystal structure of TPD-4, derived from high resolution powder diffraction techniques, is also presented and is discussed with reference to that of TPD.

Introduction

N,*N*-Diphenyl-*N*,*N*′-bis(methylphenyl)-1,1′-biphenyl-4,4′-diamines and their derivatives (Scheme 1) have been widely studied as model hole transport materials[1] and are used in multilayer systems for photocopying devices,[2] white light electroluminescent devices,[3] voltage-tunable colour organic LEDs[4] and low cost flat panel displays.[5] Pure TPD displays hole transport properties[6] but is typically incorporated into multilayer devices as a dispersion throughout a polymer support. Nevertheless, most studies still treat the hole-hopping process as an electron-transfer reaction, in a molecular material, between neighbouring neutral and radical-cation moieties.

$$N + R^{+\bullet} \rightarrow R^{+\bullet} + N \quad (1)$$

Although the structures of TPD and its cation have been studied using density functional theory[7] (DFT) in order to elucidate the changes in energy and geometry which occur during the hole-hopping process, we know of no crystallographic studies on its solid-state structure or on those of related materials. This is surprising, as these materials are used exclusively in the solid-state and the proposed intermolecular electron-transfer process is potentially highly dependent on a number of factors that can only be determined crystallographically; for example, the number and nature of intermolecular contacts, the precise conformation adopted by the molecule and the degree of freedom that the molecule has to move or to reorganise its geometry within the solid-state lattice. Diffraction studies have been carried out on triphenylamine and tritolylamine[8] which have been used as models of hole transport materials such as TPD.[9] However, Malagoli and Brédas have recently shown[7] that TPD does not reorganise in the manner of triphenylamine but that the central biphenyl moiety dominates the reorganisation process.

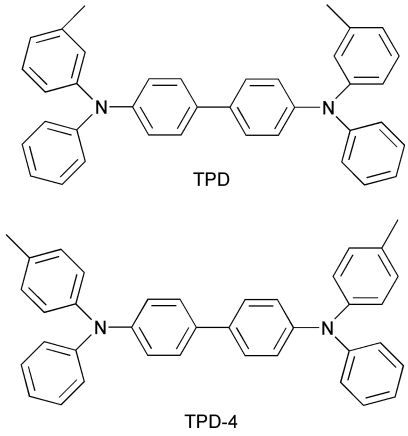

Scheme 1

Our initial strategy for structure determination was to collect high-resolution powder diffraction data on station BM16 of the European Synchrotron Radiation Facility (ESRF), using "off-the-shelf" samples of TPD and TPD-4. The rationale was to examine crystalline samples that were representative of the bulk, rather than employ recrystallisations to obtain single crystals with potentially different characteristics. Whilst TPD and TPD-4 are both relatively large molecules, they nevertheless fall within the scope of global optimisation methods of structure solution from powder diffraction data.[10] As we report below, this strategy worked well for TPD-4, but due to phase purity problems with the TPD sample, this latter structure was eventually obtained by utilising the microcrystal single crystal diffraction facility (Station 9.8) of the Daresbury SRS.[11]

 DOI: 10.1039/b107278c

Experimental

Synchrotron single crystal and powder X-ray diffraction experiments were performed on samples of TPD and TPD-4 as provided by Avecia Ltd. Laboratory based X-ray measurements were made on a sample of TPD recrystallised by slow evaporation from 2-methyltetrahydrofuran solution.

Synchrotron X-ray powder diffraction data were collected at room temperature from polycrystalline samples of TPD and TPD-4 contained in 1 mm capillaries at station BM16 of the ESRF, using an incident wavelength of 0.80008(2) Å. Whilst the diffraction data obtained from the TPD sample were extremely good, repeated attempts to index the pattern failed. Recollecting the data at 130 K, with a view to exploiting differential thermal expansion for indexing purposes, did not improve this situation. Due to constraints upon the remaining experimental time, only a very short run (total duration ~120 minutes) was possible for the TPD-4 sample. Nevertheless, an appropriate data collection scheme similar to the one described in reference 12 (see Table 1) was employed in order to improve the chances of being able to solve the structure. The data were indexed to a monoclinic cell [$a = 20.96$ Å, $b = 14.51$ Å, $c = 10.99$ Å, $\beta = 117.85°$, $V = 2958$ Å^3] using DICVOL91,[13] which returned good figures of merit, $M(20) = 41$, $F(20) = 237$. The volume of the unit cell suggested $Z = 4$ and a preliminary examination of the predicted peak positions for this cell against the measured data indicated that the space group was $P2_1/n$. Diffraction data beyond about 20° in 2θ were extremely weak and accordingly, the data used subsequently were truncated to 22° 2θ, equivalent to 2.1 Å resolution and equating to about ~60 minutes of the total data collection time. A Pawley fit to this data in $P2_1/n$ using DASH[10] gave a profile χ^2 of 3.16, with no significant misfit in the pattern, indicating that the refined unit cell and space group were correct. Further details of the Pawley fit and detailed crystallographic parameters are given in Tables 2 and 3.

The single crystal structure of TPD was calculated from measurements made on a colourless tabular crystal selected from the bulk powder sample and of approximate dimensions 120 × 60 × 60 μm. A standard Station 9.8 experiment was performed[11] using a Bruker SMART CCD detector. The structure was solved by direct methods and refined[14] to convergence on F^2. Hydrogen atoms were placed in calculated positions and in riding modes. The disordered atoms were modeled isotropically and are split over two sites whose occupancies were refined. Further crystal data and refinement parameters are given in Table 3. CCDC reference numbers 174279 and 174280. See http://www.rsc.org/suppdata/jm/b1/b107278c/ for crystallographic data in CIF format.

Laboratory single crystal X-ray data were measured on a Nonius Kappa CCD diffractometer with $\lambda = 0.71073$ Å radiation and laboratory powder X-ray diffraction data were measured at room temperature using a Bruker D8 diffractometer operating in capillary mode with $\lambda = 1.54056$ Å radiation.

Table 1 The variable count scheme used in data collection for TPD-4. Data were collected in a series of six runs, with the detector scan rate and detector sample rate set to give an equivalent step size of 0.001° 2θ. Much of the data collection time was spent in the higher-angle (>20° 2θ) region of the diffraction pattern. Note that scan 2 commenced with the central analyser crystal of the detector positioned at *minus* six degrees.

Scan	2θ Range/°	Scan rate/° min^{-1}	Sample rate/ms	Step size 2θ/°	Time/min
1	7–9.5	1	60	0.001	~2
2	−6–19	0.5	120	0.001	~50
3	3–33	2	30	0.001	~15
4	14–33	1.0	60	0.001	~19
5	24–33	0.5	120	0.001	~14
6	27–33	0.25	240	0.001	~24

Table 2 Pawley refinement parameters for TPD-4 powder data (background subtracted)

Parameter	Value
2θ minimum/°	3
2θ maximum (measured)/°	41
2θ maximum (fitted)/°	22
Effective step size	0.005
Number of points	3801
Number of reflections	335
Number of constraints	36
Number of variable intensities	307
Number of other variables	7
R_p (%)	10.8
R_{wp} (%)	11.2
R_e (%)	6.3
χ^2	3.51

Table 3 Crystallographic data and refinement parameters

	TPD (single crystal data)	TPD-4 (powder data)
Formula	$C_{38}H_{32}N_2$	$C_{38}H_{32}N_2$
MW	516.66	516.66
Crystal system	Orthorhombic	Monoclinic
a/Å	11.068(2)	20.9674(3)
b/Å	14.472(2)	14.5059(2)
c/Å	17.820(3)	10.9862(1)
β/°		117.825(2)
U/Å^3	2854.4(9)	2955.0
T/K	150	295
λ/Å	0.6892	0.8000
Space group	$P2_12_12_1$	$P2_1/n$
Z	4	4
μ/mm^{-1}	0.070	
$2\theta_{max}$/°	46	22 ($2\theta_{min} = 2$)
Reflections measured	12992	
Reflections unique	4344	
R_{int}	0.0708	
R_1	0.0668	
wR_2	0.1561	
Reflections observed	3405	335
Parameters	370	11
GoF	1.065	
R_p (%)		9.6
R_{wp} (%)		12.64
R_e (%)		3.73
Profile χ^2		10.63

Results and discussion

Theoretical structures of TPD and its cation

Malagoli and Brédas[7] performed calculations on TPD and its radical cation at the DFT level with the B3LYP functional and the 6-31G** split valence plus polarisation basis set. Their main conclusions with regard to the geometry of the two species is that neutral TPD can be viewed as mimicking its constituent parts *e.g.* a biphenyl moiety joined to two triphenylamine parts. This analogy breaks down on moving to the cation $TPD^{+\bullet}$ which retains some similarity to the corresponding biphenyl molecule but whose triarylamine region does not act like triphenylamine. The main geometric changes on moving from the neutral molecule to the cation were found to be: a shortening of the central C–C bond by approximately 0.02 Å, a flattening of the central twist between the biphenyl rings (from 33.8 to 23.0°), an asymmetry appearing in the three N–C lengths with that to the biphenyl group shortened by 0.03 Å, a decrease in the torsion angles about this N–C bond (from 42.0 to 25.8°) and an increase in the twists of the terminal phenyl

and tolyl rings (by around 7°). They also conclude that the reorganisation energy of TPD is higher than that of triphenylamine and that as it is the biphenyl moiety that dominates this reorganisation then substitution of the terminal aryl rings should have little effect on the overall reorganisation energy.

Crystal structure of TPD

The crystal structure of TPD, based on the Station 9.8 microcrystalline measurements, consists of discrete molecules separated by at least the sum of van der Waals radii. Even at 150 K the molecular structure shows a great deal of rotational movement in the four terminal aryl rings. This relative freedom of movement in the crystal lattice indicates favourable conditions for geometry reorganisation during the charge transfer process. Both the tolyl and phenyl rings attached to N1 showed sufficient movement to necessitate their modeling as split over two (closely spatially related) sites. However, the terminal rings on N2 showed a more intriguing type of disorder. It is apparent that both the rings C13 to C18 and C19 to C24 carry the methyl group for a proportion of the lattice sites. In other words a formal rotation about the C10–N2 bond relates two separate conformations of TPD which coexist in the solid-state (see Fig. 1). The occupancy of atom site C25 was refined to 70(1)% and that of atom site C25A to 30(1)% (hereafter conformations 1 and 2 respectively). Conformation 1 has both tolyl rings on the same side of both the ring planes of the central biphenyl moiety. Conformation 2 differs by having the two tolyl rings mutually *anti* with respect to these ring planes. Comparison of the core bond lengths (Table 4) from the DFT calculations and the crystal structure reveals them to be essentially identical as are the C3–C4–C7–C8 central "biphenyl" torsion angles and the planar nature of the nitrogen hybridisation. The same cannot be said for the triarylamine torsion angles. The DFT calculations predict a very symmetrical structure and identical torsion angles about both N atoms. This is certainly not the case in the crystal structure. The torsion angles given in Table 4 show that the two triarylamine fragments adopt considerably different rotational conformations. Additionally, the tolyl group attached to N1 is orientated so that its methyl group points back towards the body of the molecule whereas the tolyl group on N2 points its methyl group away from the body of the TPD molecule (see Fig. 1). The most extreme deviations between the observed and theoretical structures are the smaller C19–N2–C10–C11 angle (crystal structure −18.9(5) *vs.* DFT 42°) and the greater twist of the C10–N2–C19–C24 angle (crystal −56.3(5) and DFT 42.3° respectively). Intriguingly these values are in fact in better agreement with those calculated for the TPD radical (25.8 and 49.3°). There are two factors of significance for understanding

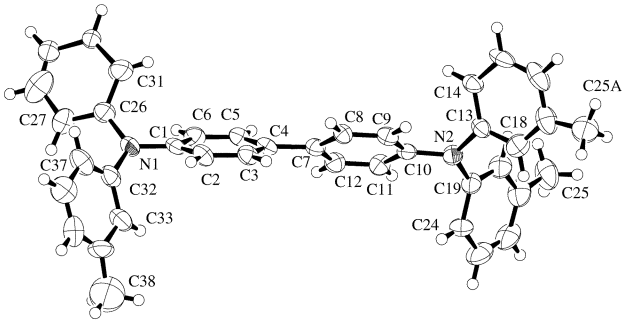

Fig. 1 The molecular structure of TPD obtained from single crystal diffraction. The rotational disorder of the terminal aromatic rings bonded to N1 is omitted for clarity. C25 is modeled at 70(1)% occupancy and C25A at 30(1)% occupancy. Non-H atoms are shown as 50% probability ellipsoids and H atoms as small spheres of arbitrary size.

Table 4 Selected bond lengths (Å) and torsion angles (°)

	TPD (crystal)	TPD (DFT)[a]	$TPD^{+\cdot}$ (DFT)[a]	TPD-4 (powder)
C4–C7	1.493(5)	1.48	1.46	
N1–C1	1.411(5)	1.42	1.39	
N1–C26	1.416(5)	1.42	1.43	
N1–C32	1.425(5)	1.42	1.43	
N2–C10	1.422(5)	1.42	1.39	
N2–C13	1.418(5)	1.42	1.43	
N2–C19	1.417(5)	1.42	1.43	
C3–C4–C7–C8	−34.7(5)	33.8	23.0	−44.5
C9–C10–N2–C13	−27.1(5)	42.0	25.8	18.5
C11–C10–N2–C19	−18.9(5)	42.0	25.8	18.5
C14–C13–N2–C10	−43.8(5)	40.6	47.6	54.6
C24–C19–N2–C10	−56.3(5)	42.3	49.3	47.0
C2–C1–N1–C32	−33.6(6)	42.0	25.8	−47.5
C6–C1–N1–C26	−44.8(6)	42.0	25.8	−47.5
C31–C26–N1–C1	−33.3(6)	40.6	47.6	−38.8
C33–C32–N1–C1	−51.8(5)	42.3	49.3	−43.5

[a]Taken from reference 7.

the energetics of the hole transport mechanism in TPD through DFT calculations. Firstly the solid-state contains two conformations of neutral TPD, neither of which corresponds to that predicted. Secondly the solid-state structure of neutral TPD displays a range of twist angles that encompass all those predicted by DFT for both the neutral and cationic forms of TPD.

Given the structure obtained from the microcrystal experiment, it is straightforward to explain why the TPD powder pattern could not be indexed (see Experimental, above). When the orthorhombic unit cell from this single crystal (Table 3) is compared to the powder data (Fig. 2), it is obvious that the bulk powder consists of at least two phases. The predominant component is identical to the $P2_12_12_1$ phase identified from the single crystal (form I) but there is a substantial quantity of additional diffracting material present. Given the chemical purity of the TPD sample and the similarity of the two diffraction patterns, this must be a second polymorph of TPD whose unit-cell dimensions we have not been able to determine. The identification of a previously unsuspected multiphase system for a material which is commercially used in the solid-state and which relies on intermolecular interactions for its utility has obvious implications.

Recrystallisation of TPD by evaporation to dryness of a 2-methyltetrahydrofuran solution produced larger crystals as colourless plates. Laboratory based powder diffraction measurements indicated that this recrystallised sample contained

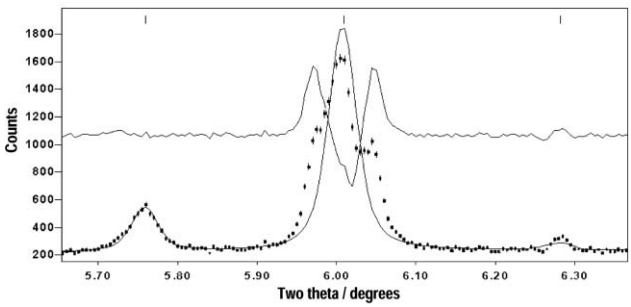

Fig. 2 Detail of the powder diffraction pattern collected on BM16 of the ESRF from a sample of TPD. The tick marks indicate the positions of the (111) , (012) and (020) reflections for the orthorhombic form I of TPD at 5.758, 6.007 and 6.281° respectively. A Pawley fit to the data using the form I cell is shown by the solid dark line, and the difference curve is shown half way up the plot as a solid faint line. This difference curve reveals the positions of reflections from a distinct contaminant phase that could not be characterized and which prevented the original determination of the structure of form I from this data alone.

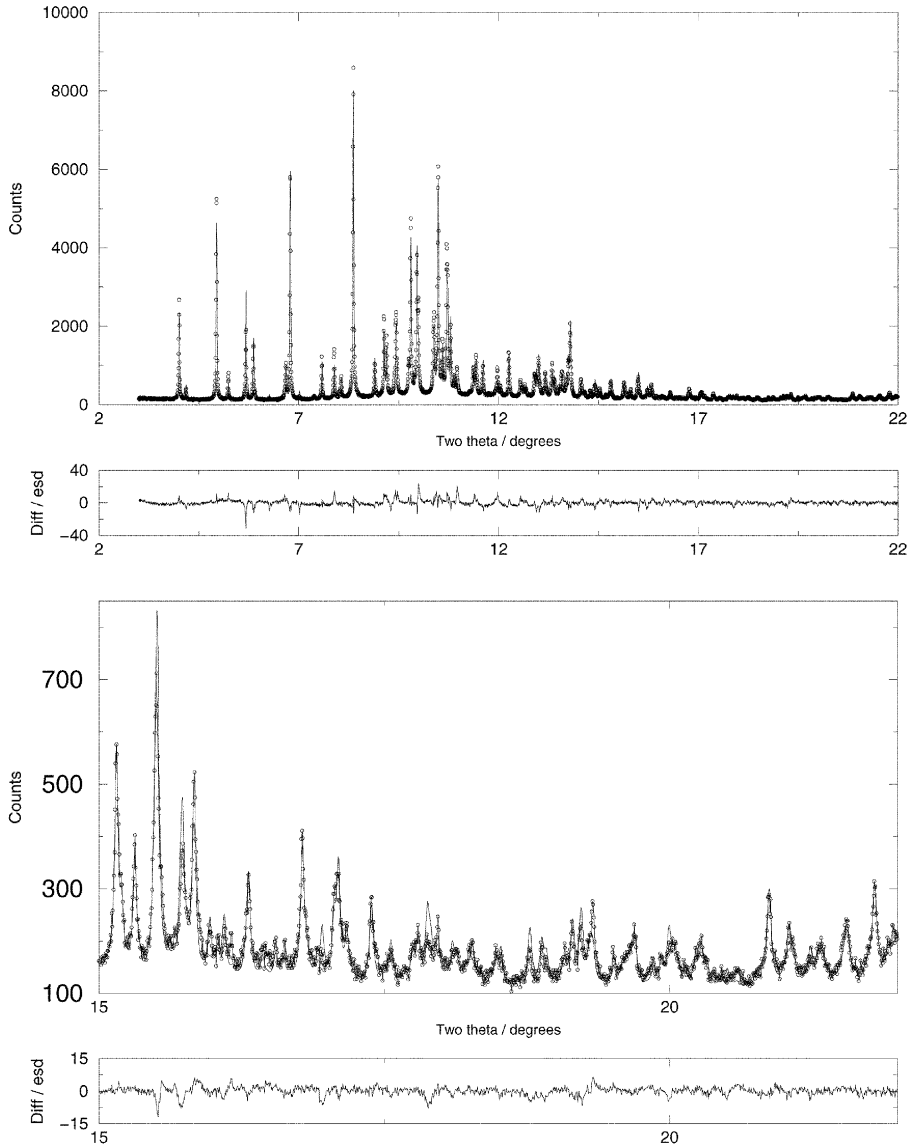

Fig. 3 Observed (small circles) and calculated (solid line) powder diffraction patterns for the crystal structure of TPD-4.

only TPD form I. Attempts were made, using a laboratory X-ray source, to obtain a single crystal structure from this sample. However, the anisotropic habit of the crystals, their small size and a marked tendency to intergrow meant that the structure solutions obtained were not of as high quality as the one obtained from Station 9.8. Nevertheless, data sets obtained both at 150 K and at 295 K supported the disordered solution reported above. The room temperature data set differed only in that the degree of rotational freedom observed was greater.

Crystal structure of TPD-4 from powder data

The TPD-4 structure was solved by the application of a global optimisation approach embodied in the DASH[10] structure solution software. An internal coordinate description of the TPD-4 molecule was constructed using standard bond lengths, bond angles and bond torsions (see Supplementary Information), resulting in a molecule whose conformation can be described in terms of only seven variable torsion angles. The position, orientation and conformation of this molecule within the refined unit cell was optimised against the measured diffraction data using eqn. (2)

$$\chi^2 = \sum_h \sum_k [(I_h - c|F_h|^2)(V^{-1})_{hk}(I_k - c|F_k|^2)] \qquad (2)$$

where I_h and I_k are Lorentz-polarisation corrected, extracted integrated intensities from a Pawley refinement of the diffraction pattern, V_{hk} is the covariance matrix from the Pawley refinement, c is a scale factor and $|F_h|$ and $|F_k|$ are the structure factor magnitudes calculated from the trial structure. At each new minimum in the intensity χ^2 space, a profile χ^2 was also calculated to facilitate comparison with the fit obtained in the Pawley refinement. Multiple optimisation runs were performed in order to ensure that the best minimum in χ^2 space had been located. About 70% of the structure solution runs returned solutions with profile χ^2 values around 11.8, with the best solution having a profile χ^2 value of 11.71. This value compares favourably with the value obtained *via* the Pawley fit ($\chi^2 = 3.5$) and suggests that the crystal structure has been correctly determined. In a further series of runs, the length of the central Ph–Ph bond was marked as a variable for optimisation but no significant improvement in the fit to the data was obtained. This length was thus fixed at 1.48 Å. Given the very limited resolution of the diffraction data obtained (2.1 Å), it is clear that only "rigid-body" refinement is appropriate. Thus, Rietveld refinement of the output DASH structural model was limited to varying only the scale factor, overall isotropic temperature factor and nine background terms which resulted in a negligible, decrease in the profile χ^2 to 10.63. There was no significant preferred orientation of the crystallites within the sample. The final Rietveld plot is shown in Fig. 3.

The conformation adopted by TPD-4 is subtly different from

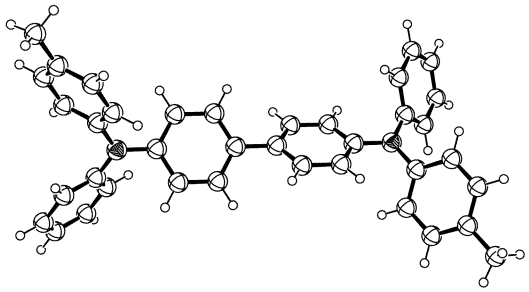

Fig. 4 The molecular structure of TPD-4 obtained from powder diffraction data.

conformation 1 of TPD which had the two tolyl rings placed *syn* with respect to both the ring planes of the two biphenyl rings and is also different to conformation 2 of TPD which displayed mutually *anti* tolyl rings. TPD-4 has an arrangement with the tolyl rings mutually *syn* with respect to the plane of one of the biphenyl rings but *anti* with respect to the other (Fig. 4). It is seen therefore that a small change in ring substitution has a marked effect on the gross molecular conformation and it has previously been shown that relatively small changes to rotational conformation can have large effects on charge transfer capabilities.[15] This is in contrast to the conclusion of reference 7 that any ring substitution in TPD type materials should have only a small influence on reorganization energies. A further difference is the larger central twist angle (-44.5 *versus* $-34.7(5)^\circ$, see Table 4) of TPD-4 as opposed to TPD. As radical cation formation seems to imply increased planarity in this region[7] this may be an unfavourable change. A similarity between this structure and that of TPD is that, despite its more symmetrical substitution, TPD-4 also has two different geometries for the triarylamine ends—as opposed to the identical geometries predicted for TPD by DFT—and again one of these is closer to the predicted cation geometry of TPD than it is to the predicted neutral geometry. The agreement between model and data is sufficiently good to suggest, but not to definitively prove, that a model containing no disorder is appropriate. This is likely to be due to the more highly symmetrical *para* substitution of TPD-4.

Conclusions

This study has characterized the bulk solid-state structures of two model hole-transport materials. Despite its relatively large molecular structure the crystal structure of TPD-4 was successfully elucidated from powder diffraction data. TPD was found to be a mixture of polymorphs. As the hole-transport and hence charge transfer mechanisms are intrinsically solid-state properties this raises the possibility of one polymorph displaying preferential properties to the other. This has a property specific and important implication for the study of the charge transport mechanism in TPD. This newly detected polymorphism also has implications for the previously measured bulk physical properties of TPD, where strict characterization of the solid-state phase is not given. The unsymmetrical nature of the molecular structures of both TPD and TPD-4 show that there is not the simple similarity between crystal structure and predicted DFT structure seen for simple analogues such as triphenylamine. Moreover the detection of two coexisting conformations in the single crystal structure of TPD, which display twist angles that encompass all those predicted by DFT for both the neutral and radical species, mean that great care must be taken when interpreting the modeling of gas phase conformations for an intrinsically solid-state phenomenon. This is especially important as charge transfer behavior has been shown to vary greatly with relatively small changes in rotational conformation.[15] Differences between gas phase and solid-state structures are often dismissed as being merely due to packing forces. This generalization may be true, but packing forces are greatly changing the ground state of the neutral TPD molecule and thus the energy differences between this and the reorganised radical cation.

Acknowledgement

The authors thank Avecia Ltd. and the EPSRC for funding a studentship (DRT) and especially Geoff Dent of that company for his ever-helpful input. We also thank BM16 station scientists Andy Fitch and Olivier Mason for their help and the ESRF and CLRC for providing beamtime awards (CH849 and 36047 respectively). We are also indebted to Alastair Florence of the University of Strathclyde for collecting laboratory powder data sets.

References

1 P. M. Borsenberger and D. S. Weiss, *Organic Photoreceptors for Xerography*, Marcel Dekker, New York, 1998.
2 D. M. Pai and B. E. Springett, *Rev. Mod. Phys.*, 1993, **65**, 163.
3 M. Strukelj, *J. Am. Chem. Soc.*, 1996, **118**, 1213.
4 J. Kalinaswki, *Appl. Phys. Lett.*, 1996, **68**, 2317.
5 V. Bulovic, G. Gu, P. E. Burrows, S. R. Forrst and M. E. Thompson, *Nature*, 1996, **380**, 29.
6 M. Stolka, J. F. Yanus and D. M. Pai, *J. Phys. Chem.*, 1984, **88**, 4707.
7 M. Malagoli and J. L. Brédas, *Chem. Phys. Lett.*, 2000, **327**, 13.
8 A. N. Sobolev, V. K. Belsky, I. P. Romm, N. Yu. Chernikova and E. N. Guryanova, *Acta Crystallogr., Sect. C.*, 1985, **41**, 967; S. L. Reynolds and R. P. Scaringe, *Cryst. Struct. Commun.*, 1982, **11**, 1129.
9 J. Pacansky, R. Waltman and H. Seki, *Bull. Chem. Soc. Jpn.*, 1997, **70**, 55.
10 W. I. F. David, K. Shankland and N. Shankland, *Chem. Commun.*, 1998, 931; W. I. F. David, K. Shankland, J. Cole, S. Maginn, W. D. S. Motherwell and R. Taylor, DASH User Manual, 2001, Cambridge Crystallographic Data Centre, Cambridge, UK.
11 R. J. Cernik, W. Clegg, C. R. A. Catlow, G. Bushnell Wye, J. V. Flaherty, G. W. Greaves, I. Burrows, D. J. Taylor, S. J. Teat and M. Hamichi, *J. Synchrotron Radiat.*, 1997, **4**, 279.
12 K. Shankland, W. I. F. David and D. S. Sivia, *J. Mater. Chem.*, 1997, **7**, 569.
13 A. Boultif and D. Louer, *J. Appl. Crystallogr.*, 1991, **24**, 987.
14 G. M. Sheldrick, SHELXS97 and SHELXL97, Programs for the solution and refinement of single crystal structures, 1997, University of Göttingen, Göttingen, Germany.
15 J. H. Slowik and I. Chen, *J. Appl. Phys.*, 1983, **54**, 4467.